PCCP

Cite this: *Phys. Chem. Chem. Phys.*, 2012, **14**, 3219–3225

www.rsc.org/pccp

PAPER

Single-molecule SERS detection of C_{60}

Camille G. Artur, Rowan Miller, Matthias Meyer, Eric C. Le Ru and Pablo G. Etchegoin

Received 4th December 2011, Accepted 9th January 2012
DOI: 10.1039/c2cp23853e

Single-molecule Surface-Enhanced Raman Scattering (SERS) detection of buckminsterfullerene (C_{60}) is achieved by using different isotopologues of the molecule with a distribution around an average isotopic substitution ($^{12}C \rightarrow {}^{13}C$) of $\sim$30%. The distribution of different isotopologues creates a broad ($\sim$20 cm^{-1}) average SERS signal within which single-molecule SERS spectra of individual isotopic realizations of the molecule can be distinguished. The SERS enhancement factors for SM-SERS C_{60} events are typically in the range of $\sim 10^8$, suggesting a limitation imposed by either photobleaching or surface interactions with the (Ag) metallic colloids to reach the highest SERS hot-spots (which can typically have larger maximum enhancements). SM-SERS signals of isotopically substituted C_{60} also show broader peaks (FWHM $\approx$ 4 cm^{-1}) than equivalent signals in natural C_{60}. The latter feature suggests a contribution to the homogeneous broadening coming from isotopic disorder in the molecule; a feature that can only be observed with the ability to detect single-molecule spectra.

Introduction and overview

Buckminsterfullerene (C_{60})[1] is arguably one of the most iconic molecules of modern times, and its physical, chemical, spectroscopic, and even environmental properties[2,3] have been studied (together with carbon nanotubes[4–9]) to an impressive level of detail.[10] Raman spectroscopy[11] of C_{60} (in its various forms) is not an exception in that sense;[12–20] and a great deal of detail on the Raman spectrum of C_{60}—with its connection to the intrinsic symmetry of the molecule and its changes under various environmental conditions[10]—is already a part of its well established properties. The intrinsic symmetry of C_{60} makes it particularly suited for the spectroscopic classification of Raman active vibrations, in terms of the different irreducible representations[21] of the icosahedral point group I_h.[18,19] It turns out that the highly symmetric character of the molecule has important consequences for its vibrational isotope effects; and this will be a key point for single molecule detection (to which we shall return later). Besides its iconic status, C_{60} finds today many applications that include being one the best known electron acceptors in organic solar cells.[22]

From the standpoint of Surface-Enhanced Raman Scattering (SERS),[23,24] a natural question arises as to whether it is possible to observe single-molecule (SM) SERS of C_{60}. After an imperfect start based on the concept of ultra-low concentrations[25,26] (normally used in single molecule fluorescence[27]) SM-SERS has now matured into a field with well established principles and procedures.[28] The problem of ultra-low concentration methods is their lack of statistical soundness,[28] which is why more reliable proofs of SM-SERS have been developed over time. The bi-analyte SERS technique introduced in ref. 29 overcomes this limitation by employing two distinguishable SERS analytes. The SM characteristics of SERS events can then be (in a statistical sense) experimentally tested.[30–32] This technique has been additionally advanced with the use of *isotopically edited molecules*.[33–36] The latter version of the technique provides two fingerprint molecules that act as mutual contrasts in the statistics of SM-events, and have exactly the same chemical properties but different Raman spectra. In the case of C_{60}, there has been to date only one report of SM-SERS detection.[37] This report, however, is based on the idea of ultra-low concentrations, as in the original papers.[25,26] Hence, the standard criticism to the original reports applies also here; *i.e.* the "rarity" of the events can be attributed to equally rare inhomogeneities in the SERS substrate and, therefore, they do not constitute by themselves a proof of SM-SERS detection. This problem is particularly acute for a molecule like C_{60}, which is non-polar, and can experience segregation or complicated surface interactions in the presence of noble metals[10] (which are typical SERS substrates). We believe that a proper demonstration of single-molecule SERS detection of C_{60} is still overdue, and one of the aims of this paper is to provide this evidence.

The objectives of our paper can be summarized as follows: (i) to provide a reliable demonstration of single-molecule C_{60} detection under SERS conditions which does *not* imply ultra-low concentrations. (ii) To quantify the range of SERS enhancement factors seen in C_{60} SM-events. This is important not only to

The MacDiarmid Institute for Advanced Materials and Nanotechnology, School of Chemical and Physical Sciences, Victoria University of Wellington, PO Box 600, Wellington, 6140, New Zealand. E-mail: Eric.LeRu@vuw.ac.nz, Pablo.Etchegoin@vuw.ac.nz

add more confidence to the result by showing that enhancement factors are in the expected range, but also to reveal whether there are additional ingredients limiting the maximum obtainable signal (like photobleaching effects[38]). Finally, (iii) to provide values for the Raman differential cross section of C_{60} for selected vibrations by comparison with a reference standard. Not only that values for the Raman differential cross sections are not hitherto available in the literature, but they are also a necessary prerequisite for the determination of the SERS enhancement factors.

Experimental

We devote first the next few subsections to some of the preliminaries that are needed to achieve the stated goals of the paper.

Differential Raman cross section

A fundamental question in SM-SERS is always that of the magnitude of the enhancement factor (EF).[39] It is well known now that credible SERS-EFs for single molecule detection cannot be above $\sim 10^9$–10^{11}.[39,40] In order to be able to quantify the SM-SERS-EF, it is necessary to: (i) ensure that the observed signals are indeed from single molecules, (ii) being able to compare the integrated peak intensity of a vibration with a signal of a known Raman differential cross section ($d\sigma/d\Omega$) under the same experimental conditions, and (iii) know the *intrinsic* $d\sigma/d\Omega$ of the molecule for that specific vibration. Unfortunately, intrinsic values of $d\sigma/d\Omega$ for a specific laser excitation are either nonexistent or very difficult to find (even for an iconic molecule like C_{60}). Therefore, we concentrate first on this task.

The easiest and most distinguishable fingerprint Raman-active vibration from C_{60} to detect single molecules is the A_g "pentagonal pinch mode" at ~ 1469 cm^{-1}.[12–20] We shall concentrate hereafter on its properties and main characteristics. The differential cross section of this mode can be obtained in solution by a direct comparison with a solvent that has a nearby Raman peak with a known $d\sigma/d\Omega$.[39] We choose to do that with toluene (which is a good solvent for C_{60}), as shown in Fig. 1, and obtain a differential cross section for the pentagonal pinch mode of $d\sigma/d\Omega = 2.9 \times 10^{-28}$ cm^2 sr^{-1}. In order to compare this value with the cross section of the free molecule (without the solvent) a local field correction for the index of refraction of toluene needs to be included.[39] This reduces the differential cross section to $d\sigma/d\Omega = 7.2 \times 10^{-29}$ cm^2 sr^{-1}, which we can use later to estimate SERS enhancement factors. We also performed DFT calculations of the cross section using *Gaussian*®, with Becke's 3-parameter hybrid functional and Lee–Yang–Parr non-local electron correlation (abbreviated as B3LYP). We used the basis set designated in *Gaussian*® as 6-311++G(d,p). The differential cross section can be readily calculated from the Raman activity produced by the program,[23] from where we obtain a theoretical value of $d\sigma/d\Omega = 9.6 \times 10^{-30}$ cm^2 sr^{-1} for the pentagonal pinch mode of C_{60}. The theoretical value is a factor of ~ 7 smaller than the experimental one, but this can be easily accounted for by an additional resonant enhancement (not included in the calculation). It is well known that C_{60} has vibronic absorptions in the visible range,[7] and these can easily contribute to a mild resonant enhancement for the cross

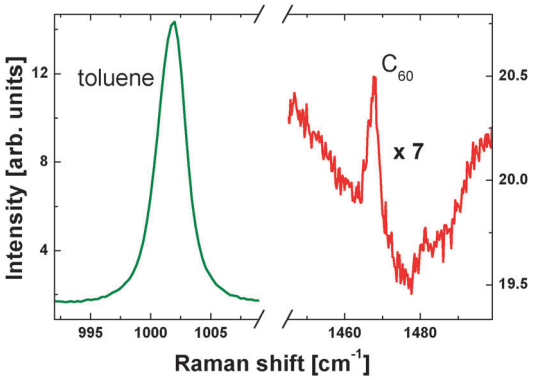

Fig. 1 Determination of the differential Raman cross section (at 633 nm laser excitation) of the 1469 cm^{-1} Raman mode of C_{60} at 1 mM concentration in toluene. The comparison is made between the known differential cross section of the 1002 cm^{-1} mode of toluene ($d\sigma/d\Omega = 2.9 \times 10^{-30}$ cm^2 sr^{-1} at 633 nm[39,41]) and the integrated intensity of the 1469 cm^{-1} pentagonal pinch mode of C_{60} (properly scaled by the number of molecules in the scattering volume and the integration time). From here we obtain $d\sigma/d\Omega = 2.9 \times 10^{-28}$ cm^2 sr^{-1} for this specific vibration (in toluene). See the text for further details.

sections compared to calculations. We use therefore the more reliable experimentally determined value for the estimation of SERS enhancement factors in what follows.

It is worth mentioning at this stage that a value of $d\sigma/d\Omega = 7.2 \times 10^{-29}$ cm^2 sr^{-1} is only a factor of ~ 10 smaller than typical cross sections for fingerprint modes of typical pre-resonant dyes used in SM-SERS. For example, the differential cross section for the 610 cm^{-1} mode of rhodamine 6G (RH6G) at 633 nm is 6.7×10^{-28} cm^2 sr^{-1},[39] and single molecules of RH6G can be easily observed with this cross section with enhancement factors of the order of $\sim 10^8$. Taking into account that maximum SERS enhancement factors can go up to $\sim 10^{10}$–10^{11}, the characterization of the differential cross section of C_{60} immediately suggests that single molecules should be detectable; except for limitations related to the ability of C_{60} to reach the right places (hot-spots) to profit from the enhancement, or additional factors linked to the photo-stability of the molecule.[38] We shall return to these points later in the paper.

Natural isotopic effect

The pentagonal pinch mode of C_{60} at ~ 1469 cm^{-1} has a very interesting natural isotopic effect. Since SM-SERS is linked sometimes to the presence of isotopologues (natural[42] or artificial[36]), it is worth mentioning the peculiar isotopic effect at this stage. The most standard stable ^{12}C isotope of carbon in any organic molecule has a $\sim 1.1\%$ chance of being replaced by ^{13}C. For the vast majority of molecules, most carbon atoms are not equivalent from the point of view of the symmetry of the molecule, and therefore the possible $^{12}C \rightarrow {}^{13}C$ substitution has a different effect on the Raman active vibrations depending on which specific carbon is actually replaced. In C_{60}, however, the irreducible representation of the pentagonal pinch mode ensures that, from the point of view of the eigenvector of the mode, all carbons are equivalent. Hence, as a result of this equivalence, we find that 34.7% of natural C_{60} will have a $^{12}C \rightarrow {}^{13}C$ substitution that produces

consistently the same isotopic shift in the frequency of the pentagonal pinch mode, and can therefore be observed as a distinct peak in a population of natural C_{60} molecules. At the same time, 11.2% of natural C_{60} will have a double $^{12}C \rightarrow {}^{13}C$ substitution. Even though the possible positions of the second carbon ^{13}C are formally (from the symmetry point of view) not equivalent for every site—because it depends on the position of the first $^{12}C \rightarrow {}^{13}C$ substitution—it turns out that the relative position of the ^{13}C atoms plays only a secondary role. The main effect on the isotopic frequency shift of the pentagonal pinch mode comes simply from the total mass substitution of ^{12}C into ^{13}C (irrespective of their relative positions). The presence of isotopically substituted C_{60} with one or two ^{13}C atoms can be observed in the Raman spectrum of the pentagonal pinch mode, in particular at low temperatures. This is explicitly shown in Fig. 2 for natural C_{60} frozen in toluene at 9 K. By freezing the C_{60} molecules into a solid transparent matrix at low temperatures we reduce additional contributions to the broadening of the peak, and a substructure of "shoulders" coming from the different natural isotopic versions of C_{60} can be revealed. The peak with three ^{13}C substitutions cannot be seen, for it has a much smaller probability of 2.4%. The independence of the exact positions of the ^{13}C substitutions on the overall frequency shift of the vibration holds also for much higher isotopic substitutions; a fact that can be demonstrated with a direct calculation of the vibrational dynamics of C_{60}; to be shown in the next subsection.

Two main key points should be highlighted from the discussion in this subsection. The first one is that, as a result of symmetry, the Raman spectrum of the pentagonal pinch mode of C_{60} is isomorphic to the isotopic mass distribution of the molecule. This fact has been studied in quite some detail by Guha *et al.*[19,20] The second point is that the frequency shift $\Delta\omega$ expected for the pentagonal pinch mode (of frequency ω_0) for a given isotopic version of C_{60} with total atomic mass m is simply given by:[10,19,20]

$$\frac{\Delta\omega}{\omega_0} = -\frac{1}{2}\frac{(m-720)}{720}, \qquad (1)$$

where 720 corresponds to the mass of C_{60} with all ^{12}C.

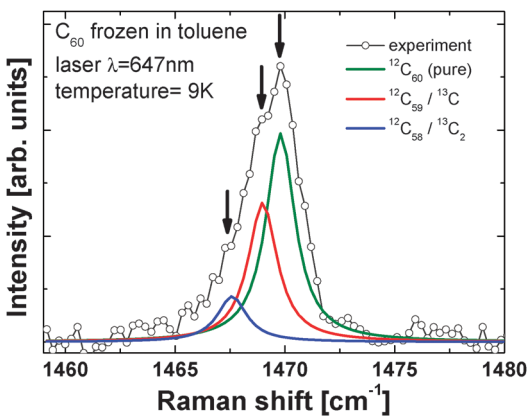

Fig. 2 Low temperature (9 K) Raman spectrum of the pentagonal pinch mode of natural C_{60} frozen in toluene (647 nm excitation line). The presence of one and two $^{12}C \rightarrow {}^{13}C$ isotopic substitutions can be seen as shoulders to the main peak of pure ^{12}C C_{60} at 1469 cm^{-1}. Due to its symmetry properties, the pentagonal pinch mode is isomorphic to the mass spectrum.[19,20]

Unfortunately, the natural isotopic effect in C_{60} cannot be used for single molecule SERS detection. The reason is that the separation among peaks is only $\sim$1 cm^{-1} according to eqn (1) (also confirmed by experimental determinations). This small shift competes with the intrinsic broadening of the peaks—which is $\sim$1.5–2 cm^{-1} (even at very low temperatures, as in Fig. 2) and the additional small frequency variations produced by the environment under SERS conditions (which is the origin of the so-called *inhomogeneous broadening* studied in ref. 43). The combination of the two effects washes out our ability to easily distinguish single isotopic versions of C_{60} differing by one mass unit.

On the other hand, it is possible to some degree to find a bi-analyte SERS[29] partner for C_{60}; and we have indeed performed experiments (not shown here) with C_{60} and 1,2-di-(4-pyridyl)-ethylene (BPE) in which we were able to distinguish individual spectra of either one compound or the other. However, the bi-analyte method[29] with two different partners works at its best when the molecules have similar chemical properties and comparable affinities for the SERS-active surface. The unique properties of C_{60} in terms of size, shape, and chemistry make it difficult to find a suitable partner; and experiments with BPE had to be performed at widely different concentrations for the two molecules (to compensate for the different surface affinity properties). This leads to a very skewed statistics of SM-events, in which the two partners might not be experiencing the same enhancement factor distributions. A much easier strategy to detect SM-SERS of C_{60} is, in fact, to *increase the isotopic spread of the natural sample* to make the different isotopic versions of the molecule more easily distinguishable despite the intrinsic homogeneous broadening of the peaks and the possible addition of small frequency shifts from the environment. This is the topic of the next subsection.

C_{60} isotopologues

Isotopically substituted C_{60} with an average of 18 sites replaced by ^{13}C has been obtained commercially (MER Corp. Tucson, AZ) and characterized by high-performance liquid chromatography (HPLC), and mass spectrometry (seen in Fig. 3(a)). The most probable atomic mass in this sample is m = 738, which implies that 18 carbons (30% of the total) have been replaced by ^{13}C. But there are (at least) 14 different isotopic variations around this most probable case, as shown in Fig. 3(a); from m = 732 to 745. We can use the mass spectrum in Fig. 3(a) as a probability distribution and calculate the histogram of possible frequencies for a large number of C_{60} molecules where the isotopic replacement sites are chosen at random. This is done with the force constants calculated by DFT in the computation we made before to obtain the Raman cross section of the pentagonal pinch mode. The DFT force constants obviously do not depend on the masses of the atoms, and can be used for any combination of isotopically substituted C_{60} with chosen random sites for ^{13}C, and a mass distribution given by the experimentally determined values in Fig. 3(a). This calculation is shown in Fig. 3(b) for 10^4 different isotopic versions of C_{60}. Note that: (i) frequencies in the calculation are overestimated with respect to experimental values (a well known fact for DFT[23,24]), and (ii) the histogram of calculated

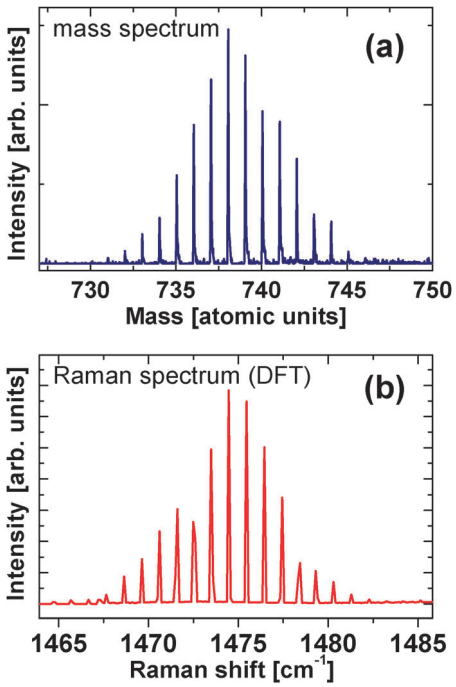

Fig. 3 (a) Experimental mass spectrum of the isotopically substituted (30% average) sample used for SM-SERS. There are (at least) 14 different isotopic substitutions around the average of 30% in the sample. (b) Vibrational Raman spectrum calculated from the DFT force constants for 10^4 random versions of isotopically substituted C_{60} chosen with a probability distribution given by the mass spectrum in (a). Because of the symmetry of the pentagonal pinch mode, the Raman spectrum is isomorphic to the mass distribution,[10,19,20] resulting in a series of discrete frequencies mimicking the mass spectrum. The Raman frequencies are overestimated in DFT calculations (a well known fact[23,24]), which is why the full spectrum appears at slightly larger frequencies than those observed experimentally in Fig. 4.

frequencies displays a series of discrete peaks mimicking the mass distribution. This *does not* happen for other vibrational modes in the molecule and it is again a manifestation of the peculiar symmetry properties of the pentagonal pinch mode and the fact that ^{13}C isotopic disorder (for a fixed number of ^{13}C) does not show an appreciable effect on the overall frequency shift (which depends then only on the total mass m). Furthermore, since the magnitude of the Raman cross section for individual isotopic realizations of C_{60} is an electronic property that does not depend on small mass-induced shifts of the frequency, the histogram of frequencies in Fig. 3(b) automatically represents the Raman spectrum of the ensemble of all possible isotopic versions of C_{60} contained in the mass spectrum of Fig. 3(a).

From the point of view of SM-SERS, the separation amongst consecutive peaks in the calculated spectrum of Fig. 3(b) is still small ($\sim$1 cm^{-1}), and might still compete to be distinct enough when the natural line widths of the peaks and the possible effects of small frequency shifts produced by the interaction with the surface[43] are taken into account. However, the existence of multiple peaks spanning a broad frequency range ($\sim$20 cm^{-1}) gives now the opportunity to spot different isotopic versions of C_{60} in SM-SERS; in what it is a natural extension of the bi-analyte SERS technique[29] to multiple (isotopic) analytes. This is the topic of the next subsection.

Single molecule detection of C_{60} isotopologues

SM-SERS experiments[30,39,43] have been carried out for the isotopic C_{60} sample excited at 633 nm and with a focus on high-resolution measurements of the pentagonal pinch mode around $\sim$1460 cm^{-1}. The samples comprised poly-L-lysine covered Si wafers, on which Ag concentrated (by centrifugation) Lee and Meisel colloids[44] were drop-casted and allowed to dry under a mild heat; thus leaving a dense collection of clusters on the surface. Small amounts of the isotopic C_{60} sample—previously dissolved in dichloromethane at 1 μM concentration—were drop casted on top of the colloids and allowed to quickly evaporate. Compared to typical concentrations used in SM-SERS experiments for resonant dyes, the C_{60} solution is very concentrated. But this is necessary to compensate for the much smaller affinity of C_{60} to stick to Ag colloids and find its place at hot-spots on the substrate. The reasonably large number of colloid clusters achieved by centrifugation together with the much higher concentration of C_{60} compared to dyes ensures that SM-SERS conditions will be found in a few selected places in the sample, as demonstrated later.

Raman spectra were acquired using a Jobin-Yvon Labram spectrometer with a $\times$100 long working distance objective (NA = 0.6) with excitation at 633 nm (2.5 mW on the sample) and a high resolution 1800 l mm^{-1} grating blazed in the red. The sample is placed inside a Linkham-Scientific THMS600 stage for optical microscopy, which keeps the sample at 77 K under a N_2 atmosphere. SM-SERS maps of 40 $\times$ 40 points (1.5 μm step and 1 s integration time per point) were taken to search for single-molecule C_{60} signals of different isotopic compositions. At least ten maps are required to obtain the necessary statistics of cases, for each map contains only $\sim$1% of clearly distinguishable SM-SERS spectra.

Fig. 4 summarizes the main SERS results. At the top of Fig. 4 we can observe the normal spectrum of natural C_{60} powder at room temperature (RT) and 633 nm excitation; with a pentagonal pinch mode at 1469 cm^{-1} and a slight broadening (and asymmetry) of the peak caused by the presence of natural isotopic substitutions (although they are not resolvable as shoulders at RT, as they were at 9 K in Fig. 2). The powder of the isotopically substituted sample (30%) at RT in Fig. 4 shows a peak with a maximum shifted to 1450 cm^{-1} (in agreement with eqn (1)), and a larger broadening than the natural sample (spanning $\sim$20 cm^{-1}) produced by the different isotopic versions of the molecule, which are revealed in the mass spectrum of Fig. 3(a). As with the natural sample, the individual isotopic versions cannot be distinguished due to the overlap and broadening of the individual peaks. The average SERS signal over 1.6 $\times$ 10^4 spectra at 77 K from the maps shows a distinct peak at approximately the same energy, but slightly narrower compared to those at RT (due to the sharpening effect of temperature on anharmonic contributions). It is worth noting that the inhomogeneous broadening of the peak in this case has its main contribution from the isotopic spread of the molecule, rather than interactions with the surface (which is the more classical contribution studied in ref. 43, and can be checked here to be $\sim$1–2 cm^{-1} in a natural C_{60} sample). By carefully sifting through the data it is possible to recover tens of single-molecule spectra per map. Examples of these spectra are given at the bottom of Fig. 4. The average of these sharp

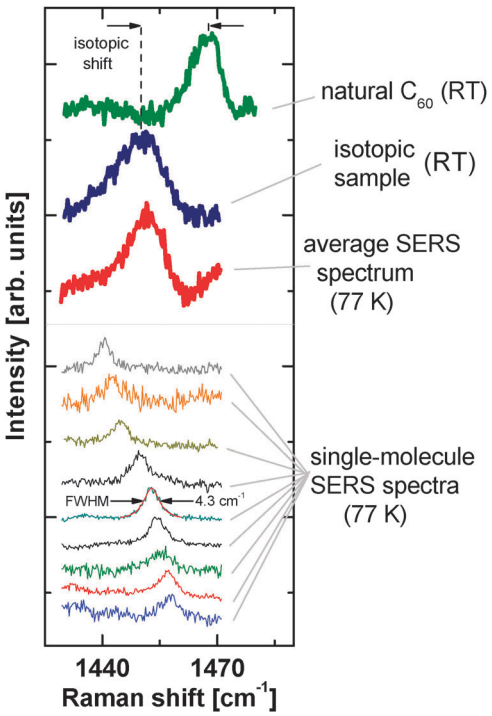

Fig. 4 The Raman spectrum of natural C_{60} (top green) at room temperature (RT) shows the pentagonal pinch mode at 1469 cm^{-1} with an additional broadening on the low energy side produced by natural isotopic substitutions. The sample with 30% average ^{13}C substitution (average mass m = 738) has the peak shifted to 1450 cm^{-1} (top blue), in agreement with eqn (1). There is an additional broadening of the peak compared with the natural sample produced by the different isotopic variations seen in Fig. 3. A linear background was subtracted from the data when present. Unlike the data at 9 K in Fig. 2, the different isotopic versions of the molecule cannot be resolved in the spectra at room temperature; neither for the natural sample nor for the isotopically substituted one. The average SERS spectrum (top red) shows a slightly narrower peak produced by a lower temperature (77 K) in which the search for an SM-SERS signal is carried out. The bottom part of the figure shows different examples of SM-SERS signals within the frequency range spanned by the average ($\sim$20 cm^{-1}). For plotting purposes the SM-spectra have been normalized to show similar intensities, but they represent in reality signals with different intensities spanning enhancement factors in the range of 6.5×10^7–1.2×10^8. In addition, SM-SERS spectra have typical broadenings in the range of $\sim$4–5 cm^{-1}, which are larger than the broadenings observed in SM-spectra of natural C_{60} at the same temperature. This is attributed to isotopic-disordered induced broadening, further discussed in the text.

SM-SERS events for all the maps recovers the average spectrum, and they span in frequency over the entire $\sim$20 cm^{-1} range where SM-SERS spectra are expected. In Fig. 4 the SM-SERS spectra have been normalized in intensity, but in reality they span a range of intensities that can be quantified into a SERS differential cross section (by comparison to a standard), and can be transformed into a SERS enhancement factor (EF) with the help of the bare differential cross section; this will be the topic of the next subsection. But, in addition, the SM-SERS spectra show characteristic widths of $\sim$4–5 cm^{-1} (as seen in Fig. 4) and this turns out to be much broader (by a factor of $\sim$2) compared to SM-SERS spectra of natural C_{60} on separate experiments—which is most of the time a molecule of pure ^{12}C—under the same experimental conditions. We attribute this interesting fact to an isotopic-disorder induced homogeneous broadening of the peak. Isotopic-disorder induced broadening is well known in crystals; including diamond which involves also combinations of ^{12}C and ^{13}C.[45] In short, our interpretation is that the isotopic disorder is a second order correction for the frequency (which only depends on the total mass), but it becomes the leading correction for the broadening by "turning on" anharmonic interactions.

Furthermore, an interesting and textbook-like aspect of spectroscopy can be revealed here. In the vast majority of cases, natural (and even artificial) isotopic effects have a very small contribution to the inhomogeneous broadening of a peak under SERS conditions, which is dominated by other environmental factors like the interaction with the surface. The latter case has been studied in detail in ref. 43, and in that framework it is possible to eke from the statistics of signals a small minority of cases where two or three molecules are seen simultaneously within the inhomogeneous broadening of a peak. Hence, these minority signals represent the simultaneous observation of a few single molecules which are distinguished in the case of ref. 43 by the different environmental conditions. In a way, the case at hand in this paper is on the opposite extreme: the main contribution to the inhomogeneous broadening of the average SERS peak in Fig. 4 is the isotopic spread of the molecules. But except for that difference, the same phenomenology applies; *i.e.* it should be possible to observe more than one molecule simultaneously which are differentiated not so much by their environmental differences but rather by different isotopic compositions. Indeed this is the case, and this is shown explicitly in Fig. 5 where minority signals from two and three molecules can be observed.

Enhancement factors

In addition to the characteristics of the SM-SERS events discussed in the previous subsection, the enhancement factors for the observed signals have to fall within an acceptable range with respect to what is known from basic electromagnetic theory.[23,39] The way to quantify them is to compare the integrated intensity of individual SM-SERS events with respect to a signal of known Raman differential cross section, under the same experimental conditions. This can be done by characterizing the effective scattering volume V_{eff} of the objective and using nitrogen (in air) as a reference. For the interested reader, the characterization procedure for the scattering volume has been explained in full detail with explicit examples of data in ref. 9 and 39. For the case at hand here, we find a scattering volume of 9.4 μm^3 for our objective, with 1.8×10^8 nitrogen molecules in it (at room temperature and normal pressure). Knowing that the 2330 cm^{-1} peak of N_2 has a differential cross section (at 633 nm excitation) of 1.6×10^{-32} cm^2 sr^{-1},[23] and normalizing by integration times with respect to the actual experiments in C_{60}, we can put numbers to the SERS cross sections of individual single molecule events. Finally, by using the experimentally determined bare cross section for the pentagonal pinch mode earlier in the paper of $d\sigma/d\Omega = 7.2 \times 10^{-29}$ cm^2 sr^{-1}, we can transform the SERS cross sections into SERS enhancement factors (EFs). The EFs depend obviously on the specific SM-SERS

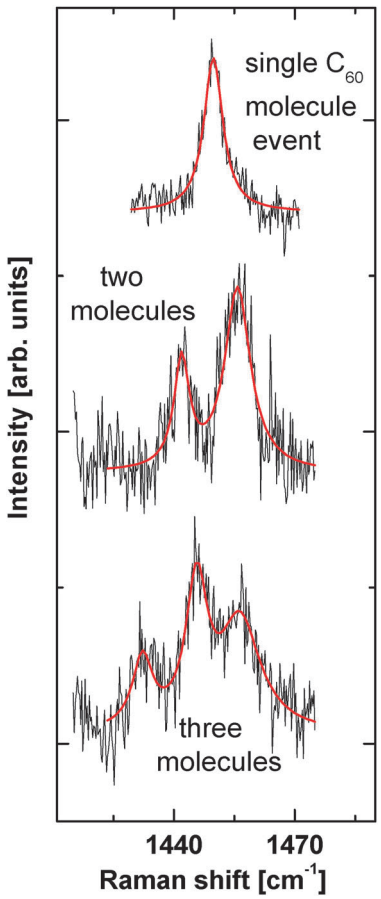

Fig. 5 SERS spectra displaying cases with different number of molecules. Unlike the results of ref. 43, where the inhomogeneous broadening is mainly created by the interaction with the surface, the isotopic spread of the molecule is the main reason for it here. Within that framework, cases with one (top), two (middle) and three (bottom) molecules can be identified in SERS maps. Cases with two or three molecules are much rarer than single molecule ones, but can be eventually identified with sufficient sampling.

event we are analyzing. The enhancement factors for the cases shown in Fig. 4, for example, range from 6.5×10^7 to 1.2×10^8. These are perfectly reasonable SM-SERS enhancement factors, comparable to those found in dyes for similar experimental conditions.[39] SM-SERS enhancement factors close to $\sim 10^{10}$–10^{11} (which are the maximum known to be compatible with electromagnetic theory) are not seen for C_{60}, but this we believe is a real effect which is either related to the photostability of the molecule[38] or its inability to find the highest-enhancement hot-spots, based on its much less favorable interaction with metallic colloids (compared to dyes) or its larger size. Similar enhancement factors were also found for single-molecule C_{60} events in the bi-analyte experiments with BPE. Overall, the range of enhancement factors, plus the spectral characteristics, and the frequency spread of the signals, all confirm and reinforce their identification as SM-SERS events of C_{60}.

Conclusions

We believe that we have provided an unequivocal proof of single molecule SERS detection of C_{60}. Besides the demonstration of single molecule detection for an iconic molecule, we believe that the results here highlight one more time the universal character of SM-SERS as a technique, which has already been demonstrated for extreme opposites in the range of cross sections (spanning from resonant dyes[39] to non-resonant and biologically relevant molecules[35]). In addition, the results in this paper show the beauty and simplicity of single molecule spectra to reveal subtle aspects of spectroscopy of molecules that would not be accessible otherwise. An example of the latter is the observation of isotopic-induced homogeneous broadening[45] in single molecule spectra. The full theoretical explanation of the isotopic-induced broadening goes beyond the harmonic approximation and is not available at present. SM-SERS provides then the experimental motivation to explain phenomena like this, which would remain hidden by ensemble averages in less sensitive types of spectroscopies.

References

1 H. W. Kroto, J. R. Heath, S. C. O'Brien, R. F. Curl and R. E. Smalley, *Nature*, 1985, **318**, 162.
2 P. R. Buseck, S. J. Tsipursky and R. Hettich, *Science*, 1992, **257**, 215.
3 J. Cami, J. Bernard-Salas, E. Peeters and S. E. Malek, *Science*, 2010, **329**, 1180.
4 S. Reich, C. Thomsen and J. Maultzsch, *Carbon Nanotubes: Basic Concepts and Physical Properties*, Wiley-VCH, Berlin, 2004.
5 R. Saito, *Physical Properties of Carbon Nanotubes*, World Scientific, Singapore, 2004.
6 *Carbon Nanotubes: Advanced Topics in the Synthesis, Structure, Properties and Applications*, ed. A. Jorio, G. Dresselhaus and M. S. Dresselhaus, Springer, Berlin, 2008.
7 M. S. Dresselhaus, M. A. Pimenta, K. Kneipp, S. D. M. Brown, P. Corio, A. Marucci and G. Dresselhaus, in *Science and Applications of Nanotubes*, Kluwer Academic/Plenum Publishers, New York, 2000.
8 S. Lefrant, J. Buisson, J. Schreiber, J. Wery, E. Faulques, O. Chauvet, M. Baibarac and I. Baltog, in *Spectroscopy of Emerging Materials*, Kluwer Academic Publishers, Amsterdam, 2004.
9 J. E. Bohn, P. G. Etchegoin, E. C. Le Ru, R. Xiang, S. Chiashi and S. Maruyama, *ACS Nano*, 2010, **4**, 3466.
10 M. S. Dresselhaus, G. Dresselhaus and P. C. Eklund, *Science of Fullerenes and Carbon Nanotubes: Their Properties and Applications*, Academic Press, New York, 1996.
11 D. A. Long, *The Raman effect, a unified treatment of the theory of Raman scattering by molecules*, John Wiley & Sons Ltd., Chichester, 2002.
12 K. A. Wang, Y. Wang, P. Zhou, J. M. Holden, S. L. Ren, G. T. Hager, H. F. Ni, P. C. Eklund, G. Dresselhaus and M. S. Dresselhaus, *Phys. Rev. B: Condens. Matter*, 1992, **45**, 1955.
13 P. C. Eklund, P. Zhou, K. A. Wang, G. Dresselhaus and M. S. Dresselhaus, *J. Phys. Chem. Solids*, 1992, **53**, 1391.
14 P. Zhou, K. A. Wang, Y. Wang, P. C. Eklund, M. S. Dresselhaus, G. Dresselhaus and R. A. Jishi, *Phys. Rev. B: Condens. Matter*, 1992, **46**, 2595.
15 S. J. Duclos, R. C. Haddon, S. H. Glarum, A. F. Hebard and K. B. Lyons, *Science*, 1991, **254**, 1625.
16 D. S. Bethune, G. Meijer, W. C. Tang and H. J. Rosen, *Chem. Phys. Lett.*, 1990, **174**, 219.
17 P. Zhou, A. M. Rao, K. A. Wang, J. D. Robertson, C. Eloi, M. S. Meier, S. L. Ren, X. X. Bi, P. C. Eklund and M. S. Dresselhaus, *Appl. Phys. Lett.*, 1992, **60**, 2871.
18 D. W. Snoke and M. Cardona, *Solid State Commun.*, 1993, **87**, 121.
19 S. Guha, J. Menéndez, J. B. Page and G. B. Adams, *Phys. Rev. B: Condens. Matter*, 1996, **53**, 13106.
20 S. Guha, J. Menéndez, J. B. Page, G. B. Adams, G. S. Spencer, J. P. Lehman, P. Giannozzi and S. Baroni, *Phys. Rev. Lett.*, 1994, **72**, 3359.
21 M. Tinkham, *Group theory and quantum mechanics*, McGraw-Hill, New York, 1964.

22 M. Campoy-Quiles, T. Ferenczi, T. Agostinelli, P. G. Etchegoin, Y. Kim, T. D. Anthopoulos, P. N. Stavrinou, D. D. C. Bradley and J. Nelson, *Nat. Mater.*, 2008, **7**, 158.
23 E. C. Le Ru and P. G. Etchegoin, *Principles of Surface Enhanced Raman Spectroscopy and Related Plasmonic Effects*, Elsevier, Amsterdam, 2009.
24 R. F. Aroca, *Surface-Enhanced Vibrational Spectroscopy*, John Wiley & Sons, Chichester, 2006.
25 S. Nie and S. R. Emory, *Science*, 1997, **275**, 1102.
26 K. Kneipp, Y. Wang, H. Kneipp, L. T. Perelman, I. Itzkan, R. R. Dasari and M. S. Feld, *Phys. Rev. Lett.*, 1997, **78**, 1667.
27 T. Plakhotnik, E. A. Donley and U. P. Wild, *Ann. Rev. Phys. Chem.*, 1997, **48**, 181.
28 P. G. Etchegoin and E. C. Le Ru, *Phys. Chem. Chem. Phys.*, 2008, **10**, 6079.
29 E. C. Le Ru, M. Meyer and P. G. Etchegoin, *J. Phys. Chem. B*, 2006, **110**, 1944.
30 P. G. Etchegoin, M. Meyer, E. Blackie and E. C. Le Ru, *Anal. Chem.*, 2007, **79**, 8411.
31 P. J. G. Goulet and R. F. Aroca, *Anal. Chem.*, 2007, **79**, 2728.
32 Y. Sawai, B. Takimoto, H. Nabika, K. Ajito and K. Murakoshi, *J. Am. Chem. Soc.*, 2007, **129**, 1658.
33 D. M. Zhang, Y. Xie, S. K. Deb, V. J. Davisson and D. Ben-Amotz, *Anal. Chem.*, 2005, **77**, 3563.
34 J. A. Dieringer, R. B. Lettan II, K. A. Scheidt and R. P. Van Duyne, *J. Am. Chem. Soc.*, 2007, **129**, 16249.
35 E. Blackie, E. C. Le Ru, M. Meyer, M. Timmer, B. Burkett, P. Northcote and P. G. Etchegoin, *Phys. Chem. Chem. Phys.*, 2008, **10**, 4147.
36 S. L. Kleinman, E. Ringe, N. Valley, K. L. Wustholz, E. Phillips, K. A. Scheidt, G. C. Schatz and R. P. Van Duyne, *J. Am. Chem. Soc.*, 2011, **133**, 4115.
37 Z. Luo, B. H. Loo, A. Peng, Y. Ma, H. Fua and J. Yao, *J. Raman Spectrosc.*, 2011, **42**, 319.
38 P. G. Etchegoin, P. D. Lacharmoise and E. C. Le Ru, *Anal. Chem.*, 2009, **81**, 682.
39 E. C. Le Ru, E. Blackie, M. Meyer and P. G. Etchegoin, *J. Phys. Chem. C*, 2007, **111**, 13794.
40 E. C. Le Ru, P. G. Etchegoin and M. Meyer, *J. Chem. Phys.*, 2006, **125**, 204701.
41 H. W. Schrötter and H. W. Klöckner, *Raman scattering cross sections in gases and liquids*, Springer, Berlin, 1979, pp. 123–166.
42 P. G. Etchegoin, E. C. Le Ru and M. Meyer, *J. Am. Chem. Soc.*, 2009, **131**, 2713.
43 P. G. Etchegoin and E. C. Le Ru, *Anal. Chem.*, 2010, **82**, 2888.
44 P. Lee and D. Meisel, *J. Phys. Chem.*, 1982, **86**, 3391.
45 J. Spitzer, P. G. Etchegoin, M. Cardona, T. R. Anthony and W. F. Banholzer, *Solid State Commun.*, 1993, **88**, 509.